Transmission Range Extension of PT-Symmetry-Based Wireless Power Transfer System

Zhihao Wei and Bo Zhang, *Senior Member, IEEE*

***Abstract*—The wireless power transfer (WPT) system based on the parity-time (PT) symmetry has been proved to be a promising WPT system due to its characteristics of constant efficiency and output power. However, the PT-symmetric range is limited, and it is necessary to widen the PT-symmetric region to extend the distance of constant and efficient transmission. The novel PT-symmetry-based WPT system with an inductor added on the receiving circuit is proposed in this article. First, the model of the proposed system is established by utilizing the coupled-mode theory, and the performance differences between the proposed system and the original PT-symmetric system are studied, and it is found that the critical coupling coefficient of the proposed system is smaller than that of the original PT-symmetric system. Second, to improve the efficiency of the proposed structure, the method of increasing the inductance of the transmitting coil is also put forward. Finally, the experimental results are basically consistent with the theoretical results, and the validity of the proposed approach is verified.**

***Index Terms*—Coupled-mode theory (CMT), coupling coefficient, parity-time (PT) symmetry, wireless power transfer (WPT).**

I. Introduction

WIRELESS power transfer (WPT) technology has been applied to some special fields, for instance, the wireless charging of electric vehicles [1]–[4], portable equipment [5]–[7], and implantable biomedical equipment [8]–[10]. At present, magnetic coupling resonance WPT technology is one of the most widely studied and applied WPT technologies [11], and it can realize midrange power transmission. However, its output power and efficiency vary with the change of coupling coefficient, and this is an inherent defect of the magnetic coupling resonance WPT technology [12]. In practical application, the relative position between the transmitting and receiving coils usually changes, and this will lead to changes in output power and efficiency; thus, the application of the technology is limited [13].

The concept of parity-time (PT) symmetry in quantum physics was introduced into WPT technology in 2017, then the problem mentioned above was solved [14]. The PT-symmetric conditions of the system are that the total gain rate and the natural resonance frequency of the transmitting circuit are equal to the total loss rate and the natural resonance frequency of the receiving circuit, respectively. When the system satisfies the PT-symmetric conditions, the output power and efficiency of the system in the PT-symmetric region are independent of the coupling coefficient, i.e., with the change of the coupling coefficient, the output power and efficiency of the system remain unchanged, and this characteristic is highly needed in WPT applications. Nevertheless, the negative resistor of the system is realized by an operational amplifier, and the output power and efficiency are low; consequently, the system is not suitable for practical situations. The problem of low output power and efficiency is addressed in [15], and it used the half-bridge inverter to realize the negative resistor; thus, the output power and efficiency of the system were increased, and it applied WPT technology based on PT symmetry to the wireless charging of drones. In [16], the PT-symmetry-based WPT system with series-parallel (SP) compensation structure is proposed. Although the transmitting and receiving circuits of the system have different topological structures, the Hamiltonian of the system is invariant after parity reflection and time-reversal operations, so the system is PT symmetry. Furthermore, the conditions for realizing the PT-symmetry-based WPT system are the two above-mentioned conditions, and the variation of operating frequency with the change of transmission distance is only one of the characteristics of the WPT system based on PT symmetry. Hence, frequency tuning is not sufficient to explain the principles and properties of the PT-symmetry-based WPT system.

The above-mentioned WPT system based on PT symmetry has strong robustness in the PT-symmetric region. However, when the coupling coefficient of the system is less than the critical coupling coefficient, i.e., the system operates in the PT-broken region, the output power and efficiency of the system are sensitive to the variation of the coupling coefficient. Therefore, it is necessary to widen the PT-symmetric range to extend the distance of constant and efficient transmission, which is also the motivation of this article.

At present, there are mainly the following ways to extend the transmission distance of the WPT system. The transmission distance can be extended by changing the coil size and structure [17], [18]. In [18], the structure of the coil adopts the eight-shaped structure, which increases the coupling coefficient between the coils, and then it can widen the transmission distance. Magnetic materials, such as ferrite, can also enhance the

Manuscript received November 20, 2020; revised February 6, 2021; accepted March 14, 2021. Date of publication March 18, 2021; date of current version June 30, 2021. This work was supported by the Key Program of the National Natural Science Foundation of China under Grant 51437005. Recommended for publication by Associate Editor M. Ponce-Silva. *(Corresponding author: Bo Zhang.)*

The authors are with the School of Electric Power Engineering, South China University of Technology, Guangzhou 510641, China (e-mail: hankwei0722@163.com; epbzhang@scut.edu.cn).

Color versions of one or more figures in this article are available at https://doi.org/10.1109/TPEL.2021.3066988.

Digital Object Identifier 10.1109/TPEL.2021.3066988

coupling between the coils, which can increase the effective transmission range [19], [20]. However, most magnetic materials will cause magnetic loss and increase the volume and weight of the system.

The transmission distance can be extended by adding repeater coils [21], [22]. However, this method will occupy a substantial amount of space along the power transmission path, so there will be certain restrictions in some applications. In addition, the transmission range can also be widened by optimizing system parameters [23], [24]. In [23], a figure-of-merit measurement method is proposed to evaluate the system performance, which can widen the effective transmission range. By increasing the inductance of the receiving coil in [24], the critical coupling coefficient is reduced, and then, the PT-symmetric range is broadened. Nevertheless, when the inductance of the receiving coil is increased, the volume of the receiving coil will enlarge. The receiving coil usually needs to be installed in electrical equipment, which has a strict restriction on the volume of the receiving coil, and this method will be limited in some applications. Besides, the receiving coil needs to be coupled with the transmitting coil to transfer energy, and its position on the receiving side is restricted, so the limited space on the receiving side cannot be fully utilized.

In order to address the above-mentioned problems and broaden the PT-symmetric region, the novel PT-symmetry-based WPT system with an inductor added to the receiving circuit is proposed in this article. First, the size of the inductor is relatively small, and it does not take up too much space. Furthermore, the inductor does not need to be coupled with the transmitting coil, and its position on the receiving side is more free, and it can make full use of the space on the receiving side. More importantly, adding an inductor can provide the additional degrees of freedom and increase the flexibility of design. The size of the receiving coil is limited by the limited space on the receiving side so that the inductance value of the receiving coil will have an upper limit. When the inductance of the receiving coil reaches the upper limit, the proposed method can further widen the PT-symmetric region.

The contributions of this article are as follows.

1) By adding an inductor to the receiving circuit, the performance of the WPT system based on PT symmetry is improved. That is, the PT-symmetric range is widened, the distance of the constant power and constant efficiency is prolonged, and the antimisalignment ability is improved.
2) The proposed WPT system with a high-order compensation structure is modeled and analyzed by the coupled-mode theory (CMT), and it is deduced that the proposed structure still satisfies the PT-symmetric conditions.
3) To improve the efficiency of the proposed method of adding an inductor only on the receiving circuit, the method of increasing the inductance of the transmitting coil while adding an inductor on the receiving circuit is also put forward. The efficiency of the proposed structure can be improved by increasing the inductance of the transmitting coil to satisfy the design requirements.
4) The influence of component tolerance on the system is analyzed, and the method of offsetting component tolerance is given. Furthermore, the design guideline of the proposed system is provided.

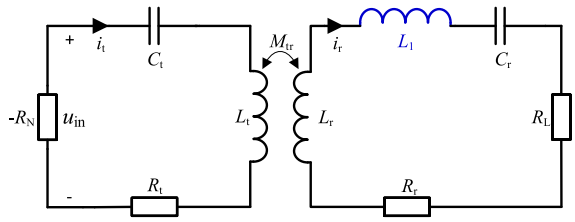

Fig. 1. Schematic diagram of the proposed WPT system based on PT symmetry.

The rest of this article is arranged as follows. In Section II, first, the proposed WPT system based on the PT symmetry is modeled and analyzed by CMT, then the relationship between the parameters of the CMT equation and the circuit parameters is obtained according to the dynamic model, and the transmission characteristics of the system are deduced. The system is designed in Section III. In Section IV, the experimental prototype of the system is constructed, then the experimental results are analyzed in detail. Finally, Section V concludes the article.

II. Principle of the Proposed WPT System Based on PT Symmetry

The schematic diagram of the proposed WPT system based on PT symmetry is shown in Fig. 1. As can be seen from Fig. 1, compared with the original WPT system based on PT symmetry, the proposed system adds an inductor to the receiving circuit. The negative resistor provides energy to the system, and it is realized by the full-bridge inverter in this article, and its specific implementation method will be described in detail in Section III.

The CMT model of the proposed WPT system based on PT symmetry can be expressed as [16], [25]

$$\frac{d}{dt}\begin{bmatrix}\boldsymbol{a}_t\\ \boldsymbol{a}_r\end{bmatrix}=\begin{bmatrix}j\omega_t+g_t & -j\kappa\\ -j\kappa & j\omega_r-\tau_r\end{bmatrix}\begin{bmatrix}\boldsymbol{a}_t\\ \boldsymbol{a}_r\end{bmatrix}. \tag{1}$$

Here, $\boldsymbol{a}_t$ and $\boldsymbol{a}_r$ are the energy modes of the transmitting and receiving circuits, respectively. ω_t and ω_r are the natural resonance angular frequencies of the transmitting and receiving circuits, respectively. g_t is the total gain rate of the transmitting circuit. τ_r is the total loss rate of the receiving circuit. κ is the coupling rate between the transmitting and receiving circuits.

When the topological structure of the WPT system changes, the CMT equation, as shown in (1), will not change, and the relationship between the parameters in the CMT equation and the circuit parameters will change. The relationship between the parameters of the CMT equation and the circuit parameters can be derived by the dynamic model, as shown in the following text.

On the basis of Fig. 1, the state equation of the WPT system with an inductor added on the receiving circuit can be obtained as

$$\begin{cases} u_{\rm in}=L_t\frac{di_t}{dt}+M_{tr}\frac{di_r}{dt}+u_{ct}+i_tR_t\\ 0=M_{tr}\frac{di_t}{dt}+(L_r+L_1)\frac{di_r}{dt}+u_{cr}+i_r\left(R_r+R_L\right)\\ i_t=C_t\frac{du_{ct}}{dt}\\ i_r=C_r\frac{du_{cr}}{dt}\end{cases} \tag{2}$$

where $u_{\rm in}$ is the ac input voltage. According to Section III, $u_{\rm in} = {\rm sgn}(i_{\rm t})V_{\rm DC}$. Here, sgn() is a sign function, and $V_{\rm DC}$ is the dc input voltage. i_t and i_r indicate the currents through the transmitting and receiving coils, respectively, and u_{ct} and u_{cr} are the voltages across compensation capacitors of the transmitting and receiving circuits, respectively. R_t is the internal resistance of the transmitting coil and R_r represents the sum of the internal resistance of the receiving coil and the internal resistance of the inductor. R_L is the load resistance. C_t and C_r are the capacitances of the compensation capacitors. L_t and L_r are the inductances of the transmitting and receiving coils, respectively, and the mutual inductance between coils is M_{tr}. L_1 is the inductance of the inductor added on the receiving circuit.

The energy modes a_t and a_r can be described as [26]

$$\begin{cases} a_t = A_t e^{j(\omega t+\theta_t)} = \sqrt{\frac{L_t}{2}} i_t + j\sqrt{\frac{C_t}{2}} u_{ct} \\ a_r = A_r e^{j(\omega t+\theta_r)} = \sqrt{\frac{L_r+L_1}{2}} i_r + j\sqrt{\frac{C_r}{2}} u_{cr}. \end{cases} \tag{3}$$

Here, ω is the operating angular frequency, A_t and A_r are the amplitudes of the energy modes, and θ_t and θ_r are the phases of the energy modes. Then, the following expression can be derived:

$$\begin{cases} u_{ct} = A_t\sqrt{\frac{2}{C_t}}\sin(\omega t+\theta_t) \\ i_t = A_t\sqrt{\frac{2}{L_t}}\cos(\omega t+\theta_t) \\ u_{cr} = A_r\sqrt{\frac{2}{C_r}}\sin(\omega t+\theta_r) \\ i_r = A_r\sqrt{\frac{2}{L_r+L_1}}\cos(\omega t+\theta_r). \end{cases} \tag{4}$$

The dynamic equations of the coupled modes can be deduced by substituting (4) into (2). Assuming that the slowly changing variables (A_t, A_r, θ_t, and θ_r) are constant during a switching period, the high-frequency terms can be ignored by the averaging method [27]. Hence, the approximate model can be expressed as

$$\frac{dA_t}{dt} = -\frac{k'A_r\omega_r}{2(1-k'^2)}\sin(\theta_t-\theta_r) + \frac{k'A_r}{(1-k'^2)}\frac{R_r+R_L}{2(L_r+L_1)} \times\cos(\theta_t-\theta_r) - \frac{A_t}{(1-k'^2)}\frac{R_t}{2L_t} + \frac{1}{(1-k'^2)}\frac{2V_{\rm DC}}{\pi\sqrt{2L_t}} \tag{5a}$$

$$A_t\left(\omega+\frac{d\theta_t}{dt}\right) = \frac{A_t\omega_t}{2(1-k'^2)} - \frac{k'A_r}{(1-k'^2)}\frac{R_r+R_L}{2(L_r+L_1)} \times\sin(\theta_t-\theta_r) + \frac{1}{2}A_t\omega_t - \frac{k'A_r\omega_r}{2(1-k'^2)}\cos(\theta_t-\theta_r) \tag{5b}$$

$$\frac{dA_r}{dt} = \frac{k'A_t\omega_t}{2(1-k'^2)}\sin(\theta_t-\theta_r) + \frac{k'A_t}{(1-k'^2)}\frac{R_t}{2L_t} \times\cos(\theta_t-\theta_r) - \frac{A_r}{(1-k'^2)}\frac{R_r+R_L}{2(L_r+L_1)} - \frac{k'}{(1-k'^2)}\frac{2V_{\rm DC}}{\pi\sqrt{2L_t}}\cos(\theta_t-\theta_r) \tag{5c}$$

$$A_r\left(\omega+\frac{d\theta_r}{dt}\right) = \frac{k'}{(1-k'^2)}\frac{2V_{\rm DC}}{\pi\sqrt{2L_t}}\sin(\theta_r-\theta_t) - \frac{k'A_t\omega_t}{2(1-k'^2)}\cos(\theta_t-\theta_r) + \frac{1}{2}A_r\omega_r + \frac{A_r\omega_r}{2(1-k'^2)} + \frac{k'A_t}{(1-k'^2)}\frac{R_t}{2L_t}\sin(\theta_t-\theta_r) \tag{5d}$$

where the natural resonance angular frequencies ω_t and ω_r can be described as $\omega_t = 1/\sqrt{L_tC_t}$ and $\omega_r = 1/\sqrt{(L_r+L_1)C_r}$, respectively. k' is a variable related to the mutual inductance $k' = M_{tr}/\sqrt{L_t(L_r+L_1)}$; in addition, the coupling coefficient of the system is $k = M_{tr}/\sqrt{L_tL_r}$. On the basis of (3), the following equation can be obtained:

$$\begin{cases} \frac{da_t}{dt} = \frac{1}{A_t}\frac{dA_t}{dt}a_t + j\left(\omega+\frac{d\theta_t}{dt}\right)a_t \\ \frac{da_r}{dt} = \frac{1}{A_r}\frac{dA_r}{dt}a_r + j\left(\omega+\frac{d\theta_r}{dt}\right)a_r. \end{cases} \tag{6}$$

Substituting (5) into (6) and ignoring higher order terms, the dynamic equations can be derived as [15]

$$\frac{d}{dt}\begin{bmatrix}\boldsymbol{a}_t\\ \boldsymbol{a}_r\end{bmatrix} = \begin{bmatrix} j\omega_t + \frac{1}{A_t}\frac{2V_{\rm DC}}{\pi\sqrt{2L_t}} - \tau_{tt} & -j\frac{\omega_r}{2}k' \\ -j\frac{\omega_t}{2}k' & j\omega_r - (\tau_{rr}+\tau_L)\end{bmatrix}\begin{bmatrix}\boldsymbol{a}_t\\ \boldsymbol{a}_r\end{bmatrix}. \tag{7}$$

Here, the inherent loss' rates of the transmitting and receiving circuits are defined as $\tau_{tt} = R_t/2L_t$ and $\tau_{rr} = R_r/2(L_r+L_1)$, respectively, and the load loss rate is defined as $\tau_L = R_L/2(L_r+L_1)$. The total loss rate of the receiving circuit is $\tau_r = \tau_{rr}+\tau_L = (R_r+R_L)/2(L_r+L_1)$. Comparing (1) with (7), it can be found that the total gain rate of the transmitting circuit is $g_t = (2V_{\rm DC}/\pi A_t\sqrt{2L_t}) - \tau_{tt}$. Since the PT-symmetric system needs to satisfy $\omega_t = \omega_r$, the coupling rate of the system is $\kappa = k'\omega_t/2$. Thus, the relationship between the parameters of the CMT equation and the circuit parameters is obtained.

When the system reaches a steady state, A_t, A_r, θ_t, and θ_r are constant. According to (1) and (3), it can be known that the operating angular frequency can be determined by the following characteristic equation:

$$\begin{vmatrix} j(\omega-\omega_t) - g_t & j\kappa \\ j\kappa & j(\omega-\omega_r)+\tau_r \end{vmatrix} = 0. \tag{8}$$

Consequently, the expression of the operating angular frequency can be described as

$$\omega = \omega_t + \alpha = \omega_t + j\frac{g_t-\tau_r}{2} \pm \sqrt{\kappa^2 - \left(\frac{g_t+\tau_r}{2}\right)^2} \tag{9}$$

where α is the real number. When $\kappa^2 = g_t\tau_r$, the operating angular frequency is $\omega = \omega_t$, and the frequency solution is unstable in the PT-symmetric region [15]. When $g_t = \tau_r$ and $\kappa > \tau_r$, the operating angular frequency is $\omega = \omega_t \pm \sqrt{\kappa^2-\tau_r^2}$, and the system works in the PT-symmetric region. According to the above-mentioned analysis, the critical coupling rate of the proposed WPT system based on PT symmetry is $\kappa_c = \tau_r$, and the corresponding critical coupling coefficient is as follows:

$$k_c = \frac{R_r+R_L}{\omega_t\sqrt{L_r(L_r+L_1)}}. \tag{10}$$

It can be seen from (10) that the critical coupling coefficient can be reduced by adding an inductor to the receiving circuit,

TABLE I
COMPARISON BETWEEN THE PERFORMANCE OF THE PROPOSED SYSTEM AND THE ORIGINAL PT-SYMMETRIC SYSTEM

	The proposed system	The original PT-symmetric system
Critical coupling coefficient	$k_c = \frac{R_r + R_L}{\omega_t \sqrt{L_r (L_r + L_1)}}$	$k_c = \frac{R_r' + R_L}{\omega_t L_r}$
Output power	$P_L = \frac{8 R_L V_{DC}^2}{\pi^2 \left[\frac{R_t (L_r + L_1)}{L_t} + R_r + R_L \right]^2} \frac{(L_r + L_1)}{L_t}$	$P_L = \frac{8 R_L V_{DC}^2}{\pi^2 \left[\frac{R_t L_r}{L_t} + R_r' + R_L \right]^2} \frac{L_r}{L_t}$
Efficiency	$\eta = \frac{R_L}{\frac{R_t (L_r + L_1)}{L_t} + (R_r + R_L)}$	$\eta = \frac{R_L}{\frac{R_t L_r}{L_t} + (R_r' + R_L)}$

TABLE II
EXPERIMENTAL PARAMETERS

Symbol	Note	Values
V_{DC}	DC input voltage	48V
ω_t , ω_r	Natural resonance angle frequency	2π×300kHz
L_t	Inductance of transmitting coil	70μH
L_r	Inductance of receiving coil	70μH
C_t	Capacitance of transmitting circuit	4.02nF
C_r	Capacitance of receiving circuit	4.02nF
R_t	Internal resistance of transmitting coil	0.25Ω
R_r'	Internal resistance of receiving coil	0.25Ω
R_L	Load resistance	10Ω

and thus, the corresponding critical transmission distance can be increased.

The amplitude of the energy mode can be derived by (1) and (7)

$$|a_t| = |a_r| = \frac{2V_{\mathrm{DC}}}{\pi\sqrt{2L_t}} \frac{1}{\tau_{tt} + \tau_r}. \tag{11}$$

On the basis of CMT, the output power of the system can be expressed as

$$P_L = 2\tau_L |a_r|^2 = \frac{4\tau_L V_{\mathrm{DC}}^2}{\pi^2 L_t (\tau_{tt} + \tau_r)^2}. \tag{12}$$

The efficiency of the proposed system can be described as

$$\eta = \frac{2\tau_L |a_r|^2}{2\tau_{tt} |a_t|^2 + 2\tau_r |a_r|^2} = \frac{R_L L_t}{(L_r + L_1) R_t + (R_r + R_L) L_t} \tag{13}$$

where $2\tau_L |a_r|^2$ is the output power, and $2\tau_{tt} |a_t|^2$ represents the power consumed by the internal resistance of the transmitting coil. $2\tau_r |a_r|^2$ is the sum of the power consumed by the internal resistance of the receiving coil, the power consumed by the internal resistance of the inductor, and the output power. It can be seen from (12) and (13) that the output power and efficiency of the system are independent of the coupling coefficient, i.e., in the PT-symmetric region, the output power and efficiency of the system remain unchanged when the distance between the transmitting and receiving coils changes.

III. SYSTEM DESIGN

A. Design of the Added Inductor

The transmission performance of the original PT-symmetric system can be obtained from the article presented in [15], and the comparison between the performance of the proposed system and the original PT-symmetric system is listed in Table I, where R_r' is the internal resistance of the receiving coil.

From the article presented in [28], the formula for calculating the number of turns of the inductor can be obtained as

$$N = \sqrt{\frac{L_1 \pi}{\mu_0 \lambda}} \tag{14}$$

where N is the number of turns of the inductor, and $\mu_0 = 4\pi \times 10^{-7}$ is the vacuum permeability. λ is a coefficient, which is related to the size of the inductor skeleton. In this article, the λ is 0.0538.

According to Wojda and Kazimierczuk [29] and Triviño-Cabrera *et al*. [30], the internal resistance of the inductor can be expressed as

$$R_w = \frac{4\rho_w l_w}{\pi s} \left(\frac{1}{d_{\mathrm{str}}^2} + \frac{\pi^3 d_{\mathrm{str}}^4 (5N_{\mathrm{ll}}^2 - 1)}{2880 \delta_w^4 p^2} \right). \tag{15}$$

Here, ρ_w is the resistivity of the winding conductor and $l_w = 2(a+b)N$ is the winding conductor length. a and b are the length and width of the skeleton, respectively. s is the number of strands of Litz wire and d_{str} represents the diameter of a single strand. $N_{\mathrm{ll}} = \sqrt{s} N_l$ is the number of winding sublayers, and N_l is the number of winding layers. $\delta_w = \sqrt{\frac{\rho_w}{\pi \mu_0 f}}$ is the skin depth of the winding conductor and f is the operating frequency. p is the distance between the center of the strands. On the basis of (14) and (15), the relationship between the internal resistance and inductance L_1 of the inductor can be acquired. Therefore, the dynamic curves of the critical coupling coefficient, output power, and efficiency of the proposed system with the change of the inductance L_1 can be drawn, as illustrated in Fig. 2. The parameters used in Fig. 2 are the same as those in Table II.

It can be found from Table I and Fig. 2 that the influence of the added inductor on the system performance is mainly reflected in three aspects. First, when an inductor is added to the receiving circuit, the critical coupling coefficient decreases and the corresponding critical transmission distance increases. Second, Table I and Fig. 2(b) show that as the inductance L_1 increases, the output power first increases sharply and then decreases slowly. Finally, as can be seen from Table I and Fig. 2(c), the efficiency decreases with the increase of inductance L_1.

The design of the added inductor mainly includes the following steps.

1) *Selection of the inductance L_1:* It can be seen from Fig. 2(a) that the rate of change of the critical coupling coefficient is relatively large when the inductance L_1 is less than 200 μH, i.e., in this interval, even if the inductance L_1 increases by a small value, the critical coupling coefficient decreases greatly. In addition, when L_1 is larger, the rate of change of the critical coupling coefficient is smaller. At this time, L_1 has less influence on the critical coupling

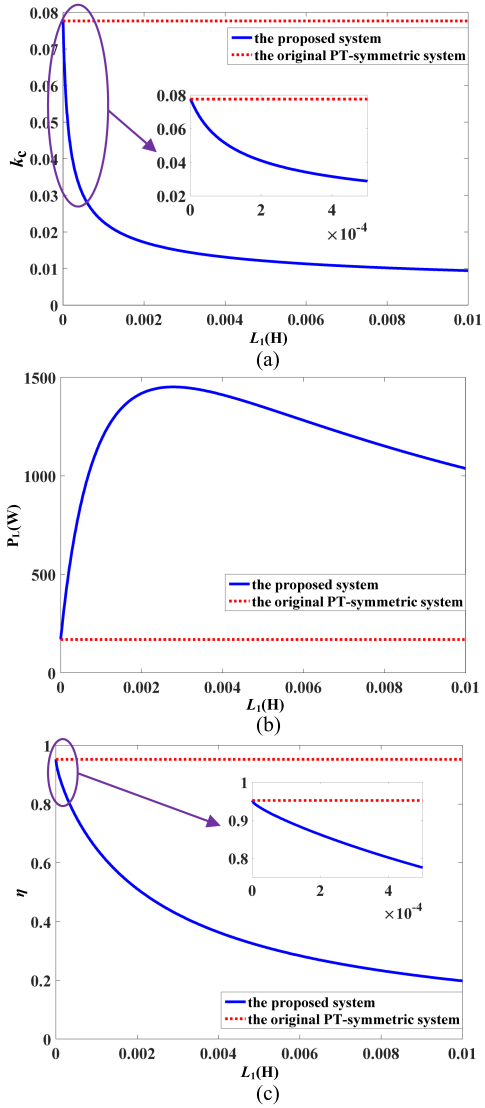

Fig. 2. Performance of the proposed WPT system based on PT symmetry. (a) Critical coupling coefficient. (b) Output power. (c) Efficiency.

coefficient. Therefore, the selection of the inductance L_1 should be less than 200 μH. The inductance L_1 of this article is set to 140 μH.

2) *Selection of the inductor type:* Inductors include the magnetic core inductors and air-core inductors. In this article, a magnetic core inductor and an air-core inductor are fabricated, respectively. For the magnetic core inductor, the N95 ferrite material of the EPCOS brand is selected, and the optimum frequency range of this material is 25–500 kHz. According to the area product method [31], the core model is selected as PQ5050, the number of turns is 39, and the air-gap length is 4.5 mm. For the air-core inductor, the skeleton is chosen as a cuboid of polybutylene terephthalate (PBT) material with a length of 64 mm, a width of 27 mm, and a height of 52 mm. Based on (14), the number of turns of the air-core inductor can be calculated as 80. Litz wire (diameter of 0.05 mm and 1000 strands) is selected to wind the magnetic core inductor and the air-core inductor. The equivalent series resistance of the magnetic core inductor is measured to be 0.59 Ω by the impedance analyzer (Wayne Kerr 6500B), and the equivalent series resistance of the air-core inductor is 0.31 Ω. Therefore, the air-core inductor is selected in this article.

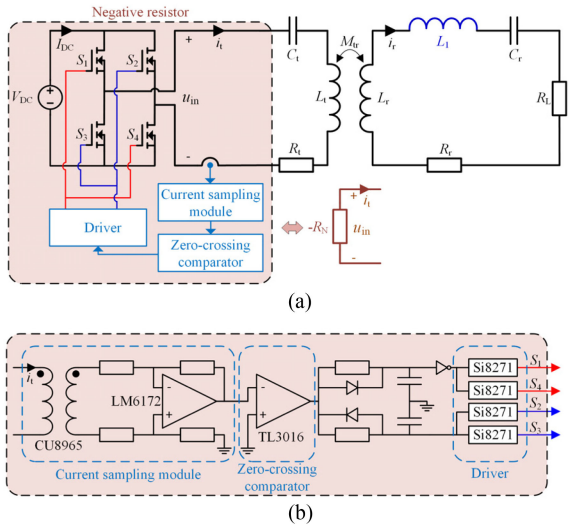

Fig. 3. Circuit diagram of the proposed WPT system based on PT symmetry.

Furthermore, it can be seen from Table I and Fig. 2 that the proposed method of adding an inductor only on the receiving circuit can prolong the transmission distance, but at the same time, the efficiency of the system will reduce. From (13), the efficiency of the system can be increased by increasing the inductance of the transmitting coil. Consequently, in order to improve the efficiency of the proposed method of adding an inductor only on the receiving circuit, the method of increasing the inductance of the transmitting coil while adding an inductor on the receiving circuit is also put forward. The efficiency of the proposed structure can be improved by increasing the inductance of the transmitting coil to meet the design requirements.

B. *Design of the Negative Resistor*

For the implementation of the entire system, the design of the negative resistor is crucial, and the negative resistor is realized by the full-bridge inverter in this article, as shown in Fig. 3. The overall circuit structure of the proposed WPT system based on PT symmetry is described in Fig. 3(a), and Fig. 3(b) shows the control circuit of the proposed WPT system. First, the current of the transmitting coil is detected by the current sense transformer (CU8965), and the detected current signal is amplified by the operational amplifier (LM6172). Second, after the signal passes through the zero-crossing comparator (TL3016), it will generate a rectangular driving signal. Finally, the driving signals pass through the drivers (Si8271) and then control the switches. The driving signals of switches S_1 and S_4 are the same, and those of switches S_2 and S_3 are identical. In addition, the driving signals of S_2 and S_3 are complementary to those of S_1 and S_4. At this time, the phase of the output voltage and output current of the

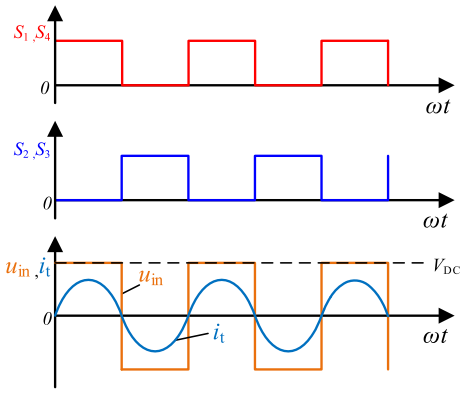

Fig. 4. Driving signal and output waveform of the full-bridge inverter.

full-bridge inverter is the same, which is equivalent to a negative resistor. The driving signal and output waveform of the full-bridge inverter are shown in Fig. 4. Therefore, the relationship between the output voltage and output current of the full-bridge inverter can be expressed as $u_{\rm in} = {\rm sgn}(i_t)V_{\rm DC}$.

IV. Experimental Verification

In order to verify the validity of the proposed method, four cases are set up in this section. Case 3 indicates the proposed method of adding an inductor only on the receiving circuit, and case 4 represents the method of increasing the inductance of the transmitting coil while adding an inductor on the receiving circuit (to improve the efficiency of case 3, case 4 is proposed). Since the coils with different inductances have different coupling coefficients at the same distance, for the fairness of the comparison, the coils of case 1 and 3 are set to be the same, and the coils of case 2 and 4 are set to be identical, where case 1 and 2 represent the original PT-symmetric system, and case 2 increases the inductance of the transmitting coil.

A. Case 1: The Experiment of the Original PT-Symmetric System

The experimental prototype of the proposed WPT system based on PT symmetry is shown in Fig. 5. The dc power supply 1 (GPS-4303C) and the dc power supply 2 (KXN-10010D) provide the dc input voltage to the system. The model of MOSFET in the full-bridge inverter is BSC098N10NS5, and its ON-state resistance is small. The compensation capacitors adopt multilayer Ceramic capacitors. Both the transmitting coil and the receiving coil are space spiral structures, and they are wound from Litz wire (diameter of 0.05 mm and 1000 strands), and the turn pitch is 3 mm. Besides, the required inductance can be obtained by adjusting the number of turns of the coil.

First, the experiment of the original PT-symmetric system is carried out. The specific experimental parameters are listed in Table II. The natural resonance frequency of the transmitting and receiving circuits is set to 300 kHz, and the operating frequency of the system will automatically track the equation $\omega = \omega_t \pm \sqrt{\kappa^2 - \tau_r^2}$ according to the change of the coupling coefficient. The inductance value of the transmitting and receiving coils is 70 μH, the number of turns is 10.7, and the coil has a radius of 150 mm and a height of 32 mm. The capacitance value of the compensation capacitor on the transmitting and receiving circuits is 4.02 nF.

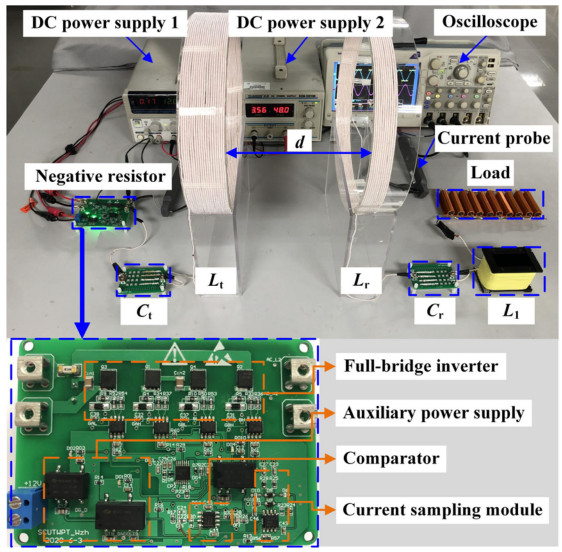

Fig. 5. Experimental prototype of the proposed WPT system based on PT symmetry.

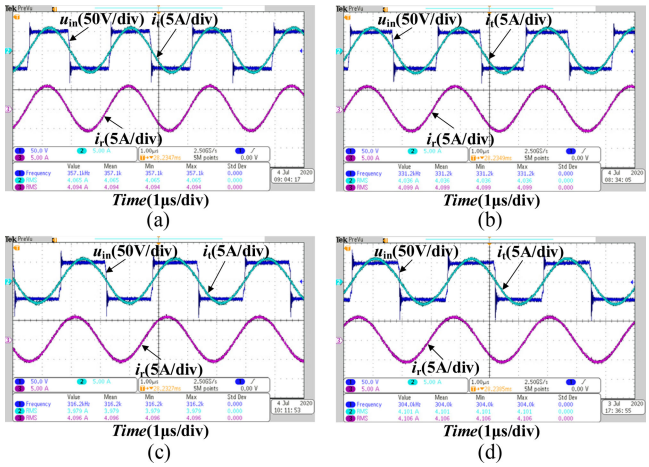

Fig. 6. Experimental waveforms of case 1 under different distances d. (a) $d = 5$ cm. (b) $d = 10$ cm. (c) $d = 15$ cm. (d) $d = 20.4$ cm.

Fig. 6 shows the experimental waveforms of case 1 under different distances. As can be seen from Fig. 6, the output voltage and output current of the full-bridge inverter have the same phase; hence, it is equivalent to a negative resistor.

The curves of transmission performance versus transmission distance for case 1 are depicted in Fig. 7. The solid line represents the theoretical result and the black point indicates the experimental result in the figure. It can be seen from Fig. 7 that the experimental results are basically consistent with the theoretical

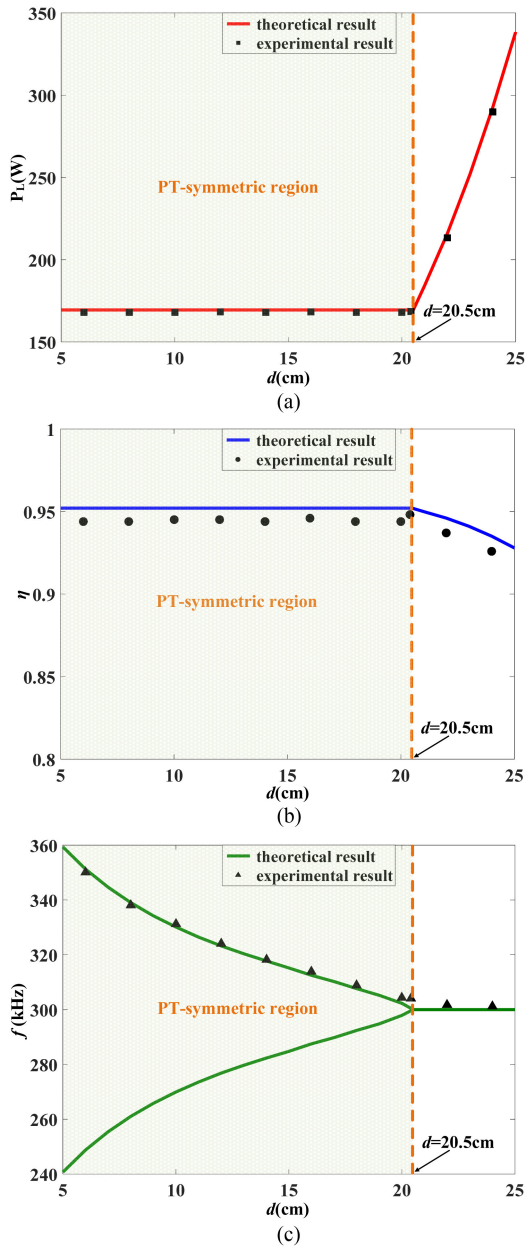

Fig. 7. Curves of transmission performance versus transmission distance for case 1. (a) Output power. (b) Efficiency. (c) Operating frequency.

results. The theoretical value of the critical transmission distance is 20.5 cm, and the theoretical value of the corresponding critical coupling coefficient is 0.0777. The experimental value of the critical transmission distance is 20.4 cm, and the experimental value of the corresponding critical coupling coefficient is 0.0782. Here, the relationship between the transmission distance and the coupling coefficient is measured by the impedance analyzer. When transmission distance d is less than 20.4 cm, the output power and efficiency of the system remain basically unchanged. At this time, the system works in the PT-symmetric region. When the transmission distance increases from 10 to 20 cm, the operating frequency decreases by about 28 kHz, and the operating frequency varies widely.

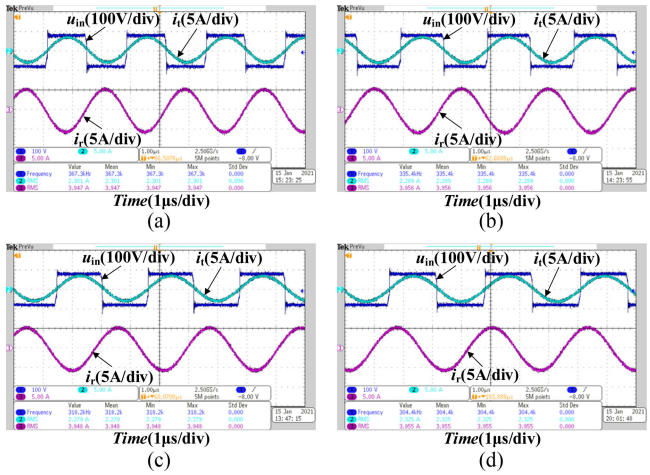

Fig. 8. Experimental waveforms of case 2 under different distances d. (a) $d = 5$ cm. (b) $d = 10$ cm. (c) $d = 15$ cm. (d) $d = 21.3$ cm.

B. Case 2: The Experiment of Only Increasing the Inductance of the Transmitting Coil

Second, the experiment of only increasing the inductance of the transmitting coil is carried out. The inductance value of the transmitting coil is 210 μH, the number of turns is 20.8, the coil has a radius of 150 mm and a height of 62 mm, and its internal resistance is 0.4 Ω. The capacitance value of the transmitting circuit is 1.34 nF. To compare the efficiency at the same output power, the input voltage is set to 79 V. Other experimental parameters are identical to those in Table II.

The experimental waveforms of case 2 under different distances are described in Fig. 8, and Fig. 9 shows the curves of transmission performance versus transmission distance for case 2. As can be seen from Fig. 9, the theoretical and experimental values of the critical transmission distance are 21.3 cm, and the theoretical and experimental values of the corresponding critical coupling coefficient are 0.0777. When the transmission distance increases from 10 to 21 cm, the operating frequency decreases about 32 kHz.

C. Case 3: The Experiment of Adding the Inductor Only

Third, without changing the inductance of the transmitting coil, the experiment of adding an inductor only on the receiving circuit is carried out. The inductance value of the added inductor on the receiving circuit is 140 μH, the inductor has a length of 76 mm, a width of 39 mm, and a height of 52 mm, and the internal resistance of the inductor is 0.31 Ω. The capacitance value of the compensation capacitor on the receiving circuit is 1.34 nF. To compare the efficiency at the same output power, the input voltage is set to 29 V. Other experimental parameters are the same as those in Table II.

The experimental waveforms of case 3 under different distances are depicted in Fig. 10. The curves of transmission performance versus transmission distance for case 3 are shown in Fig. 11. As can be seen from Fig. 11, the theoretical and experimental results are basically identical. The theoretical value of the critical transmission distance is 26.6 cm, and the theoretical

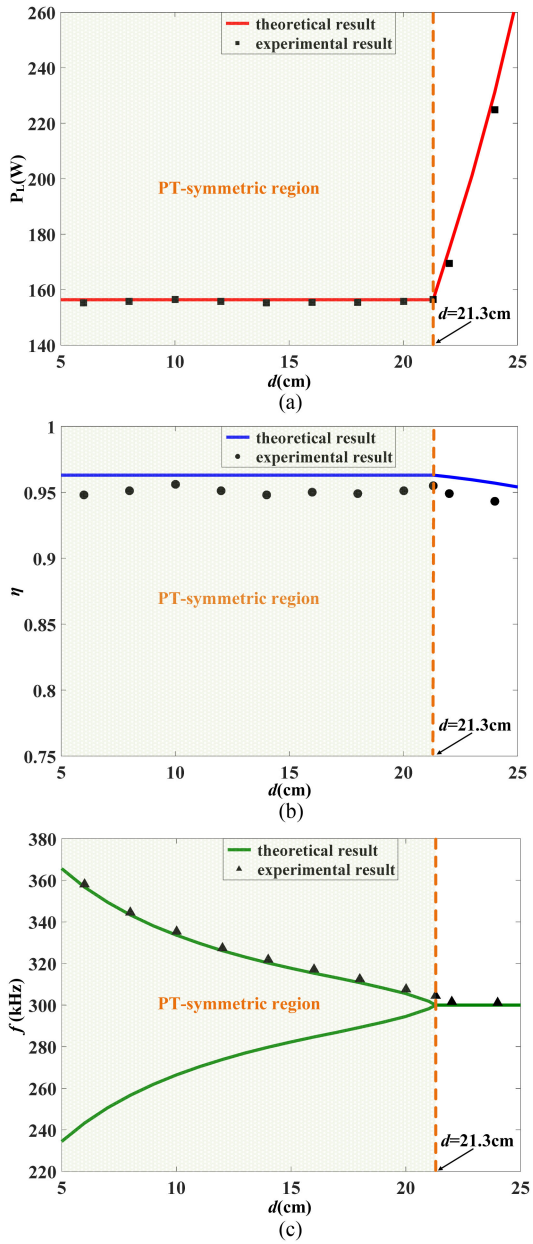

Fig. 9. Curves of transmission performance versus transmission distance for case 2. (a) Output power. (b) Efficiency. (c) Operating frequency.

value of the corresponding critical coupling coefficient is 0.0462. The experimental value of the critical transmission distance is 26.6 cm, and the experimental value of the corresponding critical coupling coefficient is 0.0462. When transmission distance d is less than 26.6 cm, the output power and efficiency of the system remain basically unchanged. When the transmission distance increases from 10 to 26 cm, the operating frequency reduces about 17 kHz. Compared with case 1, the critical transmission distance of case 3 is extended by 30.4%. Therefore, the method of adding an inductor to the receiving circuit can extend the distance of the constant power and constant efficiency.

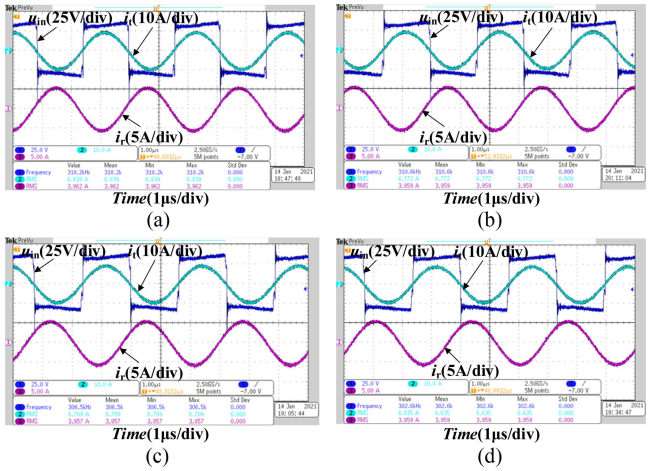

Fig. 10. Experimental waveforms of case 3 under different distances d. (a) $d = 10$ cm. (b) $d = 15$ cm. (c) $d = 20$ cm. (d) $d = 26.6$ cm.

D. Case 4: The Experiment of Adding the Inductor and Increasing the Inductance of the Transmitting Coil at the Same Time

Finally, the experiment of increasing the inductance of the transmitting coil while adding an inductor to the receiving circuit is carried out. The inductance value of the added inductor on the receiving circuit is 140 μH, and the inductance value of the transmitting coil is 210 μH. The capacitance value of the compensation capacitor on the transmitting and receiving circuits is 1.34 nF. Other experimental parameters are identical to those in Table II.

The experimental waveforms of case 4 under different distances are described in Fig. 12, and Fig. 13 shows the curves of transmission performance versus transmission distance for case 4. The theoretical value of the critical transmission distance is 27.3 cm, and the theoretical value of the corresponding critical coupling coefficient is 0.0462. The experimental value of the critical transmission distance is 27.5 cm, and the experimental value of the corresponding critical coupling coefficient is 0.0460. When transmission distance d is less than 27.5 cm, the output power and efficiency of the system remain basically constant. When the transmission distance increases from 10 to 27 cm, the operating frequency decreases about 19 kHz. Compared with case 2, the critical transmission distance of case 4 is prolonged by 29.1%; thus, the method of adding an inductor on the receiving circuit can widen the PT-symmetric region. Furthermore, compared with case 3, the efficiency of case 4 is increased by 3.2%; hence, increasing the inductance of the transmitting coil can improve the efficiency of the proposed structure.

In order to clearly compare the system performance of the above four cases in the PT-symmetric region, the theoretical and experimental results of the critical coupling coefficient, corresponding critical transmission distance, output power, and efficiency under different situations are listed in Table III. In addition, the experimental values of the output power and efficiency in Table III are the average values measured.

TABLE III
SYSTEM PERFORMANCE OF THE DIFFERENT CASES

	Critical coupling coefficient (Theoretical /Experimental)	Critical transmission distance(cm) (Theoretical /Experimental)	Output power(W) (Theoretical /Experimental)	Efficiency (Theoretical /Experimental)
Case 1	0.0777/0.0782	20.5/20.4	169.4/168.1	95.2%/94.5%
Case 2	0.0777/0.0777	21.3/21.3	156.4/155.7	96.3%/95.1%
Case 3	0.0462/0.0462	26.6/26.6	159.9/156.7	88.4%/87.4%
Case 4	0.0462/0.0460	27.3/27.5	155.5/155.1	91.2%/90.6%

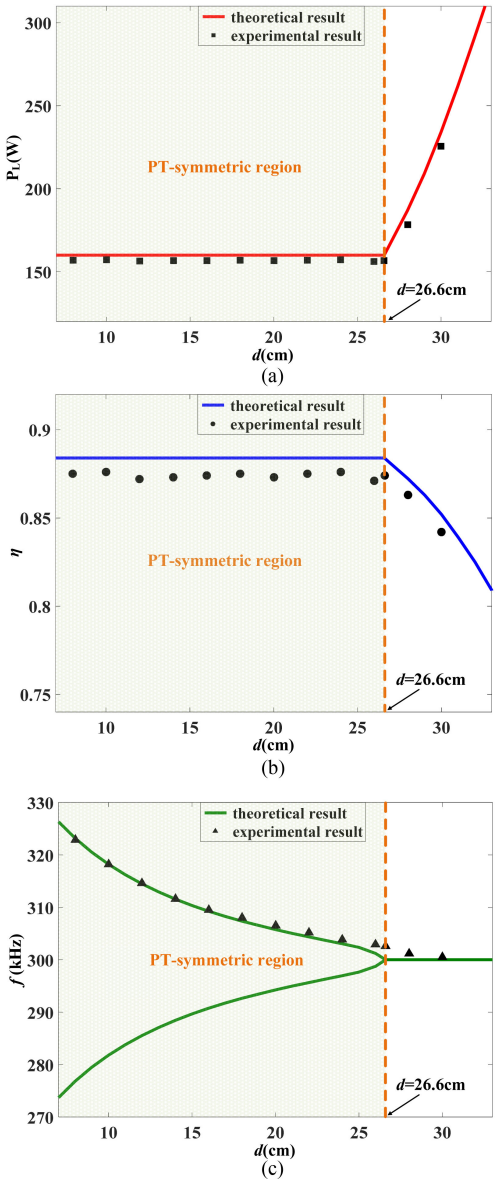

Fig. 11. Curves of transmission performance versus transmission distance for case 3. (a) Output power. (b) Efficiency. (c) Operating frequency.

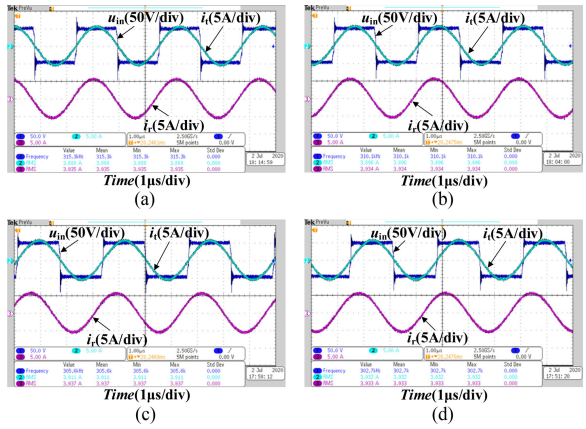

Fig. 12. Experimental waveforms of case 4 under different distances d. (a) $d = 15$ cm. (b) $d = 20$ cm. (c) $d = 25$ cm. (d) $d = 27.5$ cm.

E. Power Loss Analysis

The rms values of the output voltage and current of the inverter are measured by an oscilloscope, and then the output active power of the inverter can be calculated. The input voltage and current of the inverter are directly read from the dc power supply 2, and then the input power of the inverter can be calculated. The inverter loss is obtained by subtracting the output power of the inverter from the input power of the inverter. Furthermore, the coil loss and inductor loss are obtained by the same measurement method (input active power minus output active power).

Fig. 14 shows the power loss of the WPT system under different cases. It can be seen from Fig. 14(a) that, in case 1, the power loss of the system mainly includes the coil loss and the inverter loss. The efficiency of the system is 94.5%, and the total loss of the system is 9.8 W. The coil loss is 7.5 W, which accounts for 76.5% of the total loss, and the inverter loss is 2.3 W, which accounts for 23.5% of the total loss. As can be seen from Fig. 14(b) that, in case 2, the efficiency of the system is 95.1%, and the total loss of the system is 8.0 W. The coil loss is 5.8 W, which accounts for 72.5% of the total loss, and the inverter loss is 2.2 W, which accounts for 27.5% of the total loss. It can be found from Fig. 14(c) that, in case 3, the power loss of the system mainly includes the coil loss, the inverter loss, and the inductor loss. The efficiency of the system is 87.4%, and the total loss of the system is 22.6 W. The coil loss is 15.0 W, which accounts for 66.4% of the total loss, the inverter loss is 2.9 W, which accounts for 12.8% of the total loss, and the inductor loss is 4.7 W, which accounts for 20.8% of the total loss. Fig. 14(d) indicates that, in case 4, the efficiency of the system is 90.6%, and the total loss of the system is 16.1 W. The coil loss is 9.2 W, which accounts for 57.1% of the total loss, the inverter loss is 2.3 W, which accounts

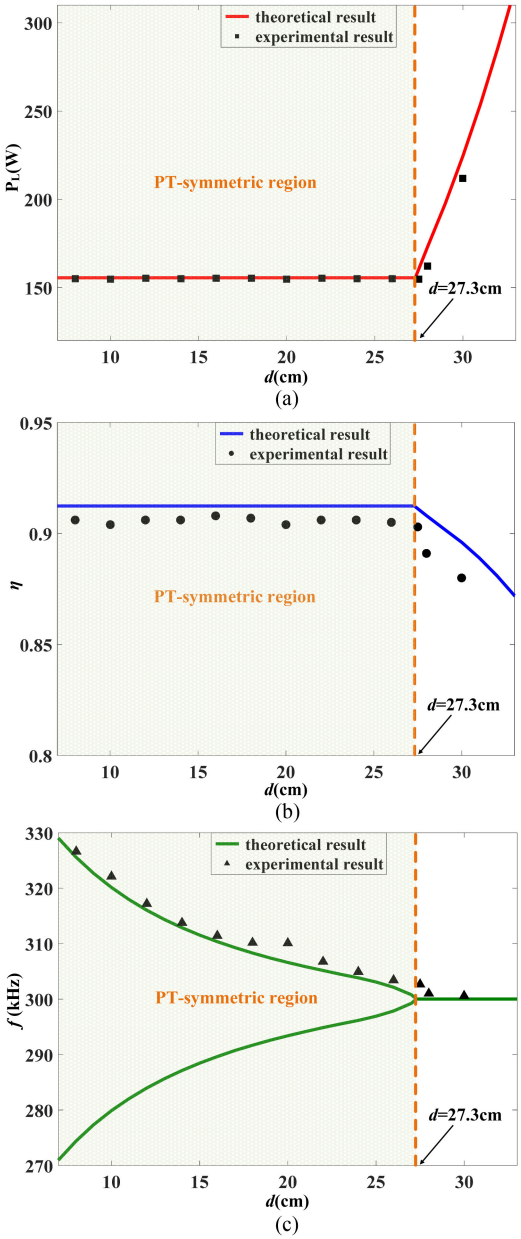

Fig. 13. Curves of transmission performance versus transmission distance for case 4. (a) Output power. (b) Efficiency. (c) Operating frequency.

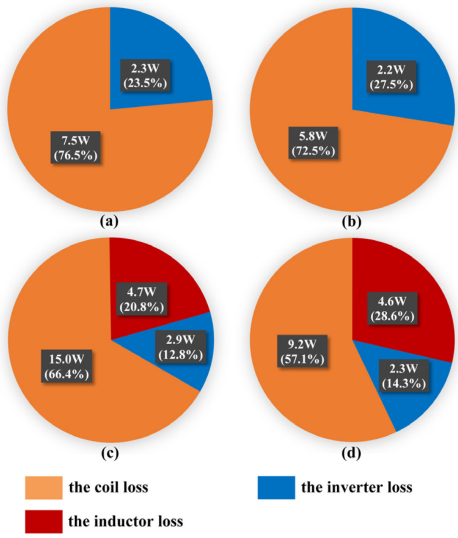

Fig. 14. Power loss of the WPT system under different cases. (a) Case 1. (b) Case 2. (c) Case 3. (d) Case 4.

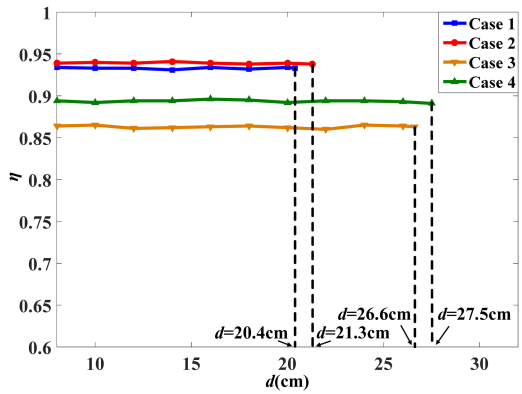

Fig. 15. Efficiency from dc input to dc output for all cases.

for 14.3% of the total loss, and the inductor loss is 4.6 W, which accounts for 28.6% of the total loss.

It has to be mentioned that the experimental prototype of this article is mainly used to verify the validity of the proposed method. The auxiliary power supply of the prototype is provided by the dc power supply 1, and the power consumed by the auxiliary power supply is small, so then the loss of the auxiliary power supply is not considered in the power loss analysis.

Furthermore, the negative resistor is realized by the full-bridge inverter in this article. The loss of the negative resistor is similar to that of the traditional power inverter, which is mainly the loss of the MOSFET. That is, the loss of the negative resistor is the inverter loss, and the negative resistor does not bring additional loss.

F. Efficiency From DC Input to DC Output

In many applications, the dc output is required to power the load. Therefore, the efficiency from dc input to dc output is measured. The model of the diode in the rectifier is SBR40U100CT. The relationship between the dc load resistance R_o and the input resistance R_L seen into the rectifier can be expressed as [32] $R_L = 8R_o/\pi^2$. When R_L is 10 Ω, the dc load resistance R_o is 12.34 Ω. Hence, the resistance of the dc electronic load (Chroma 63115A) is set to 12.34 Ω. The efficiency from dc input to dc output for all cases is shown in Fig. 15.

As can be seen from Fig. 15, in the PT-symmetric region, the efficiency from dc input to dc output of case 1 is 93.3%, and the overall efficiency of case 2 is 93.9%. The efficiency from dc input to dc output of case 3 is 86.3%, and the overall efficiency of case 4 is 89.4%. Compared with case 3, the overall efficiency of case 4 is increased by 3.1%. Therefore, increasing the inductance of the transmitting coil can improve the efficiency of the proposed structure to satisfy the design requirements of efficiency in practical applications.

G. Experiment of Increasing the Inductance of the Receiving Coil

In order to compare the method of increasing the inductance of the receiving coil and the proposed method of adding an inductor only on the receiving circuit (case 3), the experiment of increasing the inductance of the receiving coil is carried out. The inductance of the transmitting coil is 70 μH, and the inductance of the receiving coil is 210 μH. The capacitance value of the compensation capacitor on the transmitting circuit is 4.02 nF, and the capacitance value of the compensation capacitor on the receiving circuit is 1.34 nF. The input voltage is set to 29 V.

In the method of increasing the inductance of the receiving coil, the theoretical value of the critical transmission distance is 33.8 cm, the theoretical value of the corresponding critical coupling coefficient is 0.0263, and the theoretical value of the efficiency is 89.7%. The experimental value of the critical transmission distance is 33.9 cm, the experimental value of the corresponding critical coupling coefficient is 0.0263, and the experimental value of the efficiency is 88.3%.

When the inductance of the receiving coil is increased from 70 to 210 μH, the volume of the system increases by 2120.6 cm^3, and the critical transmission distance is extended by 13.5 cm, i.e., in the method of increasing the inductance of the receiving coil, when the volume is increased by 1 cm^3, the critical transmission distance is prolonged by 0.00637 cm. As can be seen from case 3, when an inductor with an inductance value of 140 μH is added to the receiving circuit, the volume of the system increases by 154.1 cm^3, and the critical transmission distance is prolonged by 6.2 cm. That is, in the proposed method of adding an inductor only on the receiving circuit, when the volume is increased by 1 cm^3, the critical transmission distance is extended by 0.0402 cm. Consequently, in the case of increasing the same volume, the proposed approach can extend a long distance.

H. Influence of the Component Tolerance

In the WPT system, the component tolerances mainly include coil tolerance and capacitor tolerance, which mainly affect the natural resonance frequency of the system. The component tolerances will cause the natural resonance frequency to shift, which will cause the system to detune.

Taking case 4 as an example, the effect of frequency detuning on the system efficiency is studied. The natural resonance frequency of the transmitting circuit remains unchanged, which is 300 kHz. In order to simulate the frequency detuning ($\omega_t \neq \omega_r$), this article changes the natural resonance frequency of the receiving circuit by adjusting the compensation capacitance of the receiving circuit. Fig. 16 shows the system efficiency curves when the natural resonance frequencies of the receiving circuit are 300, 302, 304, and 308 kHz, respectively. According to the equation $\omega_r = 1/\sqrt{(L_r + L_1)C_r}$, when the natural resonance frequency of the receiving circuit is 308 kHz, the compensation capacitance is 1.27 nF. Compared with 1.34 nF (the natural resonant frequency of the receiving circuit is 300 kHz), the equivalent error of the compensation capacitance is 5.2%. It can be found from Fig. 16 that the acceptable component error of the proposed system is 2.6% (the natural resonant frequency of the receiving circuit is 304 kHz), and the component error has little effect on the system at this time. It has to be mentioned that for other forms of WPT systems, component tolerances have the same restriction [14].

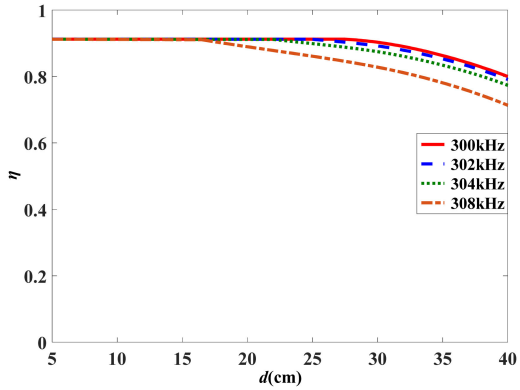

Fig. 16. Effect of frequency detuning on system efficiency.

Fortunately, the error of each capacitor can be offset by paralleling multiple capacitors, which is also the method used in this article to reduce the capacitor error. For instance, the capacitor with a capacitance value of 4.02 nF, in this article, is formed by connecting four 1 nF capacitors and two 10 pF capacitors in parallel.

I. Application Value and the Design Guideline

The proposed method (adding an inductor on the receiving circuit) can decrease the critical coupling coefficient of the system and broaden the PT-symmetric region. In the PT-symmetric range, the output power and efficiency of the system are independent of the coupling coefficient. That is to say, the proposed approach can not only prolong the distance of the constant power and constant efficiency but also improve the antimisalignment ability of the system. Therefore, the proposed structure can be applied to scenarios with high requirements for transmission distance and antimisalignment ability.

The specific applications are as follows.

1) *Electric rice cooker, electric kettle, and other kitchen electrical equipment:* In this application, the transmitting side of the WPT system is usually installed under the desktop, and the receiving side is installed in the kitchen appliance. The thickness of each user's desktop is different. When the desktop is very thick, consumers have high requirements for the transmission distance. In addition, the coil misalignment is inevitable when users use the appliance; hence, consumers also have high requirements for the antimisalignment ability. The above requirements may not be satisfied by optimizing the system parameters (for example, the transmission distance is extended by increasing the inductance of the receiving coil. The receiving coil is usually installed in the base of the kitchen appliance, and the base space is limited, so the inductance of the receiving coil has an upper limit). At this time, an inductor can be added to the receiving circuit to further reduce the critical coupling coefficient. So, then the distance of constant and

efficient transmission is extended, the antimisalignment ability is improved, and the requirements of consumers are met. The added inductor does not need to be coupled with the transmitting coil, and its position on the receiving side is more flexible so that the limited space of the receiving side can be fully utilized.

2) *Wireless charging of the electric vehicle:* Different types of electric vehicles have different heights from the ground to the chassis, and sport utility vehicles and buses have high requirements for transmission distance. For the wireless charging station of electric vehicles, it needs to charge different types of electric vehicles, so then it is vital that the output power and efficiency remain unchanged at different distances. Furthermore, it is difficult for drivers to accurately park their car above a designated charging point; thus, drivers also have high requirements for the antimisalignment ability. The proposed method can broaden the PT-symmetric region to satisfy these requirements.
3) *Wireless charging of the unmanned underwater vehicle:* Since the existence of waves in the ocean, the relative position between the coils constantly changes during the charging process. That is, the coupling coefficient of the system varies constantly. In order to ensure the stable output of the wireless charging system for underwater equipment, the wireless charging system is required to have strong antimisalignment ability. Hence, the proposed system is very suitable for this application scenario.

Furthermore, to satisfy the design requirements of the transmission distance and efficiency in practical application, the design guideline of the proposed structure is as follows.

1) *Calculation of the maximum inductance of the receiving coil:* The diameter and height of the receiving coil can be obtained from the space reserved for the coil by the system, so the maximum inductance of the receiving coil can be calculated based on the article presented in [28].
2) *Calculation of the inductance of the added inductor:* According to Neumann's formula [33], the coupling coefficient with various transmission distances can be calculated. Therefore, the corresponding critical coupling coefficient can be acquired based on the highest design requirements of the transmission distance. The inductance of the added inductor can be calculated from (10).
3) *Adjusting the inductance of the transmitting coil:* Finally, to satisfy the design requirements of efficiency, the inductance of the transmitting coil is adjusted according to (13). So far, the design of system parameters has been completed.

V. Conclusion

In this article, the novel PT-symmetry-based WPT system with an inductor added to the receiving circuit is proposed. The critical coupling coefficient, output power, and efficiency of the proposed WPT system based on PT symmetry are derived by utilizing CMT. The critical coupling coefficient of the proposed system is smaller than that of the original PT-symmetric system, i.e., the PT-symmetric region of the proposed system is larger than that of the original PT-symmetric system. To improve the efficiency of the proposed structure, the method of increasing the inductance of the transmitting coil while adding an inductor to the receiving circuit is also put forward. The experimental prototype is built. Compared with case 1, the critical transmission distance of case 3 is prolonged by 30.4%. Compared with case 2, the critical transmission distance of case 4 is extended by 29.1%. Hence, the proposed method of adding an inductor to the receiving circuit can extend the distance of constant and efficient transmission. Furthermore, compared with case 3, the efficiency of case 4 is increased by 3.2%. Therefore, the efficiency of the proposed structure can be improved by increasing the inductance of the transmitting coil to satisfy the design requirements. Finally, the application value and the design guideline of the proposed structure are discussed, and the proposed structure can be applied to scenarios with high requirements for transmission distance and antimisalignment ability.

References

[1] D. H. Tran, V. B. Vu, and W. Choi, "Design of a high-efficiency wireless power transfer system with intermediate coils for the on-board chargers of electric vehicles," *IEEE Trans. Power Electron.*, vol. 33, no. 1, pp. 175–187, Jan. 2018.

[2] Z. Luo and X. Wei, "Analysis of square and circular planar spiral coils in wireless power transfer system for electric vehicles," *IEEE Trans. Ind. Electron.*, vol. 65, no. 1, pp. 331–341, Jan. 2018.

[3] Y. Jiang, L. Wang, Y. Wang, J. Liu, M. Wu, and G. Ning, "Analysis, design, and implementation of WPT system for EV's battery charging based on optimal operation frequency range," *IEEE Trans. Power Electron.*, vol. 34, no. 7, pp. 6890–6905, Jul. 2019.

[4] Y. Huang, C. Liu, Y. Zhou, Y. Xiao, and S. Liu, "Power allocation for dynamic dual-pickup wireless charging system of electric vehicle," *IEEE Trans. Magn.*, vol. 55, no. 7, Jul. 2019, Art. no. 8600106.

[5] J. Park *et al.*, "A resonant reactive shielding for planar wireless power transfer system in smartphone application," *IEEE Trans. Electromagn. Compat.*, vol. 59, no. 2, pp. 695–703, Apr. 2017.

[6] J. Moon, H. Hwang, B. Jo, C.-K. Kwon, T.-G. Kim, and S.-W. Kim, "Design and implementation of a high-efficiency 6.78-MHz resonant wireless power transfer system with a 5-W fully integrated power receiver," *IET Power Electron.*, vol. 10, no. 5, pp. 577–587, Nov. 2016.

[7] W. Zhang *et al.*, "High-efficiency wireless power transfer system for 3D, unstationary free-positioning and multi-object charging," *IET Electr. Power Appl.*, vol. 12, no. 5, pp. 658–665, May 2018.

[8] Y. Lu, D. Qiu, X. Meng, B. Zhang, and S. C. Tang, "S-PS resonant topology of WPT system for implantable spinal cord stimulator," *IET Power Electron.*, vol. 11, no. 15, pp. 2499–2506, Dec. 2018.

[9] X. Meng, D. Qiu, M. Lin, S. C. Tang, and B. Zhang, "Output voltage identification based on transmitting side information for implantable wireless power transfer system," *IEEE Access*, vol. 7, pp. 2938–2946, 2019.

[10] H. Zhang, S.-P. Gao, T. Ngo, W. Wu, and Y.-X. Guo, "Wireless power transfer antenna alignment using intermodulation for two-tone powered implantable medical devices," *IEEE Trans. Microw. Theory Techn.*, vol. 67, no. 5, pp. 1708–1716, May 2019.

[11] A. Kurs, A. Karalis, R. Moffatt, J. D. Joannopoulos, P. Fisher, and M. Soljacic, "Wireless power transfer via strongly coupled magnetic resonances," *Science*, vol. 317, no. 5834, pp. 83–86, Jul. 2007.

[12] J. Zhou, B. Zhang, G. Liu, and D. Qiu, "Resonance and distance insensitive wireless power transfer with parity-time symmetric duffing resonators," in *Proc. IEEE Wireless Power Transfer Conf.*, Montreal, QC, Canada, 2018, pp. 1–4.

[13] Z. Zhang and B. Zhang, "Omnidirectional and efficient wireless power transfer system for logistic robots," *IEEE Access*, vol. 8, pp. 13683–13693, 2020.

[14] S. Assawaworrarit, X. Yu, and S. Fan, "Robust wireless power transfer using a nonlinear parity–time-symmetric circuit," *Nature*, vol. 546, no. 7658, pp. 387–390, Jun. 2017.

[15] J. Zhou, B. Zhang, W. Xiao, D. Qiu, and Y. Chen, "Nonlinear parity-time-symmetric model for constant efficiency wireless power transfer: Application to a drone-in-flight wireless charging platform," *IEEE Trans. Ind. Electron.*, vol. 66, no. 5, pp. 4097–4107, May 2019.

[16] S. Assawaworrarit and S. Fan, "Robust and efficient wireless power transfer using a switch-mode implementation of a nonlinear parity–time symmetric circuit," *Nature Electron.*, vol. 3, no. 5, pp. 273–279, May 2020.
[17] M. Kavitha, P. B. Bobba, and D. Prasad, "Effect of coil geometry and shielding on wireless power transfer system," in *Proc. IEEE 7th Power India Int. Conf.*, Bikaner, India, 2016, pp. 1–6.
[18] W.-X. Chen and Z.-P. Chen, "Optimization on the transmission distance and efficiency of magnetic resonant WPT system," in *Proc. CSAA/IET Int. Conf. Aircr. Utility Syst.*, Guiyang, China, 2018, pp. 148–154.
[19] F. Y. Lin, A. Zaheer, M. Budhia, and G. A. Covic, "Reducing leakage flux in IPT systems by modifying pad ferrite structures," in *Proc. IEEE Energy Convers. Congr. Expo.*, Pittsburgh, PA, USA, 2014, pp. 1770–1777.
[20] M. Wang, J. Feng, Y. Shi, and M. Shen, "Demagnetization weakening and magnetic field concentration with ferrite core characterization for efficient wireless power transfer," *IEEE Trans. Ind. Electron.*, vol. 66, no. 3, pp. 1842–1851, Mar. 2019.
[21] K. Phaebua, T. Lertwiriyaprapa, S. Chalermwisutkul, and P. Akkaraekthalin, "Area extension of a wireless battery charging system using multiple power repeater coil antennas," in *Proc. 2nd Int. Conf. Intell. Green Building Smart Grid*, Prague, Czech Republic, 2016, pp. 1–4.
[22] J. Barreto, A.-S. Kaddour, and S. V. Georgakopoulos, "Conformal strongly coupled magnetic resonance systems with extended range," *IEEE Open J. Antennas Propag.*, vol. 1, pp. 264–271, Jun. 2020.
[23] C.-W. Yang and C.-L. Yang, "Analysis of inductive coupling coils for extending distances of efficient wireless power transmission," in *Proc. IEEE MTT-S Int. Microw. Workshop Ser. RF Wireless Technol. Biomed. Healthcare Appl.*, Singapore, 2013, pp. 1–3.
[24] W. Dong, C. Li, H. Zhang, and L. Ding, "Wireless power transfer based on current non-linear PT-symmetry principle," *IET Power Electron.*, vol. 12, no. 7, pp. 1783–1791, Jun. 2019.
[25] H. A. Haus, *Waves and Fields in Optoelectronics*. Englewood Cliffs, NJ, USA: Prentice-Hall, 1984.
[26] H. Li, K. Wang, L. Huang, W. Chen, and X. Yang, "Dynamic modeling based on coupled modes for wireless power transfer systems," *IEEE Trans. Power Electron.*, vol. 30, no. 11, pp. 6245–6253, Nov. 2015.
[27] J. A. Sanders and F. Verhulst, *Averaging Methods in Nonlinear Dynamical Systems*. New York, NY, USA: Springer, 1985.
[28] T. Chen, B. Liu, Y. Luo, and Y. Zhang, *Inductance Calculation Manual*. Beijing, China: China Machine, 1992.
[29] R. P. Wojda and M. K. Kazimierczuk, "Winding resistance and power loss of inductors with litz and solid-round wires," *IEEE Trans. Ind. Appl.*, vol. 54, no. 4, pp. 3548–3557, Jul./Aug. 2018.
[30] A. Triviño-Cabrera, J. M. González-González, and J. A. Aguado, *Wireless Power Transfer For Electric Vehicles: Foundations and Design Approach*. Cham, Switzerland: Springer, 2020.
[31] M. K. Kazimierczuk and H. Sekiya, "Design of AC resonant inductors using area product method," in *Proc. IEEE Energy Convers. Congr. Expo.*, San Jose, CA, USA, 2009, pp. 994–1001.
[32] Y. Li, T. Lin, R. Mai, L. Huang, and Z. He, "Compact double-sided decoupled coils-based WPT systems for high-power applications: Analysis, design, and experimental verification," *IEEE Trans. Transp. Electrific.*, vol. 4, no. 1, pp. 64–75, Mar. 2018.
[33] F. Liu, Y. Yang, D. Jiang, X. Ruan, and X. Chen, "Modeling and optimization of magnetically coupled resonant wireless power transfer system with varying spatial scales," *IEEE Trans. Power Electron.*, vol. 32, no. 4, pp. 3240–3250, Apr. 2017.

Zhihao Wei was born in Shandong, China, in 1990. He received the B.S. and M.S. degrees in electrical engineering from Qingdao University, Qingdao, China, in 2015 and 2018, respectively. He is currently working toward the Ph.D. degree in power electronics and power drives with the School of Electric Power, South China University of Technology, Guangzhou, China.

His research interests include wireless power transfer technology and fractional-order system.

Bo Zhang (Senior Member, IEEE) was born in Shanghai, China, in 1962. He received the B.S. degree in electrical engineering from Zhejiang University, Hangzhou, China, in 1982, the M.S. degree in power electronics from Southwest Jiaotong University, Chengdu, China, in 1988, and the Ph.D. degree in power electronics from the Nanjing University of Aeronautics and Astronautics, Nanjing, China, in 1994.

He is currently a Professor with the School of Electric Power, South China University of Technology, Guangzhou, China. He has authored or coauthored more than 450 papers and held 102 patents. He has also authored eight monographs. His research interests include nonlinear analysis and control of power electronics, wireless power transfer technology, and ac drives.